The unusual 2020 Arctic ozone hole as seen in the CAMS reanalysis

A. Inness[1], S. Chabrillat[2], J. Flemming[1], V. Huijnen[3], B. Langenrock[2], J. Nicolas[1], I. Polichtchouk[1] and M. Razinger[1]

[1]ECMWF, Shinfield Park, Reading, RG2 9AX, UK.

[2]Royal Belgian Institute for Space Aeronomy (BIRA-IASB), Ringlaan 3, 1180 Brussels, Belgium

[3]Royal Netherlands Meteorological Institute, De Bilt, the Netherlands.

Corresponding author: Antje Inness (a.inness@ecmwf.int)

Key Points:

- Arctic ozone columns in spring 2020 were the lowest since 1979
- The Artic polar vortex in spring 2020 was unusually strong, cold and long lasting with reduced wave driving from the troposphere
- Profiles from limb sounding satellites show clear signs of chlorine activation and the presence of polar stratospheric clouds over the Arctic in March 2020
- The CAMS reanalysis captures stratospheric ozone well and shows good agreement with ozone sondes reproducing the low Arctic ozone values in late March and early April 2020

Abstract

A reanalysis dataset produced by the Copernicus Atmosphere Monitoring service (CAMS reanalysis, 2003 - present day) augmented by ERA5 data for the years before 2003 is used to describe the evolution of the 2020 Arctic ozone season and to compare it with years back to 1979. Ozone columns over large parts of the Arctic reached record low values in March and April 2020 because of an exceptionally cold and persistent Arctic polar vortex. Minimum ozone columns were below 250 DU for most of March and the first half of April, with the lowest values of 211 DU in the CAMS reanalysis found on 18 March. Such low values are extremely unusual for the Arctic. The previous years with similarly strong Arctic ozone depletion were 2011 and 1997 with minimum values of 232 DU and 217 DU, respectively. The performance of the CAMS ozone analysis is assessed by comparison with ozone sonde data. We find a clear sign of chemical ozone destruction with ozone severely depleted in a layer between 80-50 hPa in late March and early April when partial pressure values below 2 mPa were observed. Profiles from the limb sounders ACE-FTS and MLS show clear signs of chlorine activation and the presence of polar stratospheric clouds. Monthly mean ozone columns in March 2020 were up to 180 DU or 40% lower than the CAMS climatology (2003-2019) while values for 2011 and 1997 were lower by 31% and 35% respectively.

Plain Language Summary

The stratosphere is the layer of the atmosphere between about 15-50 km where most of the ozone resides. Usually, Arctic ozone reaches maximum values in the stratosphere during boreal spring. However, in spring 2020 the Arctic stratosphere was exceptionally cold, and ozone transport from the mid-latitudes was inhibited. Because of the low temperatures, polar stratospheric clouds could form over the Artic region and lead to stratospheric ozone destruction. This led to record low ozone columns in the Arctic at the end of March and the beginning of April 2020, with minimum values of 211 DU. This is lower than in 1997 and 2011, the previous two years that had exceptionally low ozone columns over the Arctic during spring. In spring 2020, the Arctic ozone layer showed clear signs of chemical ozone depletion with ozone almost completely destroyed in a layer around 18 km in a way that is usually only seen over the Antarctic during the austral spring, when the ozone hole forms. We can therefore talk about an Arctic ozone hole in spring 2020.

1 Introduction

While we are used to ozone holes developing over the Antarctic every year during Austral spring (World Meteorological Organization (WMO), 2018), the conditions that are needed for such strong ozone depletion are normally not found in the Northern Hemisphere (NH). There, the winter-time polar vortex is usually weaker and more perturbed than in the Southern Hemisphere (SH), and stratospheric temperatures are not as low as over the Antarctic during austral winter and spring (Waugh et al., 2017). This is the result of greater planetary wave activity in the NH (Shepherd, 2008) because of the larger topographic and land-sea contrast than in the SH. These waves can propagate upwards in the winter hemisphere when stratospheric winds are westerly and dissipate in the upper stratosphere (‘wave breaking’) decelerating the Arctic polar vortex and leading to a warmer and more perturbed Arctic stratosphere (Garcia and Boville, 1994). Because the Arctic polar vortex is less stable than the Antarctic one, more mixing occurs between the Arctic and ozone-richer midlatitudes than in the SH (Manney et al., 1994).

The wave drag also drives a poleward transport in the stratosphere from the ozone source regions in the tropics, with connected downward transport in the extratropics and upward transport in the tropics, as part of the large-scale overturning Brewer Dobson circulation (Brewer, 1949; Dobson, 1956). Because the wave activity is stronger in the NH during winter/spring than in the SH, the Brewer-Dobson circulation is not symmetric in both hemispheres (Shepherd, 2008) but leads to a stronger build-up of ozone in the lower stratosphere at high northern latitudes during boreal spring than in the SH during austral spring. The downward transport at high latitudes also leads to adiabatic warming and overall higher temperatures in the lower stratosphere of the NH than the SH. Consequently, fewer polar stratospheric clouds (PSCs) form in the Arctic stratosphere during winter/spring resulting generally in less severe catalytic ozone depletion than in the SH during austral winter/spring.

Typical total column ozone (TCO3) values at the beginning of winter are around 450 DU in the NH but only around 330 DU in the SH (WMO, 2018). Consequently, even if severe chemical ozone depletion happened in the Arctic the resulting ozone columns would be larger than the very low values (below 100 DU) that were found in some years over the Antarctic (see NASA's Ozone Watch https://ozonewatch.gsfc.nasa.gov/meteorology/annual_data.html). Manney et al. (2011) argue that ozone values below 250 - 275 DU in the Arctic during winter are exceptional and can be referred to as a NH ozone hole even though 220 DU is the usual SH ozone hole threshold.

Ozone columns over large parts of the Arctic reached record low values below 250 DU in March and April 2020 with ozone severely depleted in a layer between 80-50 hPa between mid-March and mid-April 2020. The last time similarly low ozone columns were observed over the Arctic was during boreal spring 2011 (Manney et al, 2011) and 1997 (Newman et al., 1997). Lawrence et al. (2020) showed that the record breaking strong polar vortex in winter/spring 2020 developed as a combination of weak wave driving from the troposphere and a wave-reflecting configuration in the upper stratosphere. The 2020 Arctic polar vortex was cold enough to allow PSCs to form, leading to large stratospheric ozone losses.

The Copernicus Atmosphere Monitoring Service (CAMS, atmosphere.copernicus.eu), operated by the European Centre for Medium-Range Weather Forecasts (ECMWF) on behalf of the European Commission, provides daily analyses and 5-day forecasts of atmospheric composition, including analyses of stratospheric ozone in near-real time (NRT). CAMS followed the evolution of the 2020 Arctic ozone depletion in NRT making use of the full 3-dimensional ozone analysis fields to assess the evolution of the TCO3 field as well as the vertical structure of the ozone field. In addition to providing daily NRT analyses and forecasts, CAMS also produces a reanalysis of atmospheric composition (Inness et al., 2019), which covers the years from 2003 onwards and again includes stratospheric ozone. This reanalysis uses a single version of the CAMS model and data assimilation system, taking care to minimize changes in the versions of the used emissions or assimilated satellite retrievals. It is now running close to NRT and allows us to intercompare recent years and to derive anomalies against climatologies calculated over the whole period of the CAMS reanalysis (2003-2019) while avoiding spurious effects from changes in the model and the assimilation system.

In this paper, we use ozone data from the CAMS reanalysis to document the evolution of the 2020 Arctic ozone field, as well as stratospheric temperatures and zonal winds, and compare stratospheric ozone during the Arctic winter and spring 2019/2020 with other years covered by the CAMS reanalysis. We use data from the ERA5 reanalysis (Hersbach et al., 2020) to extend

the TCO3 timeseries back to 1979 and assess the performance of the CAMS reanalysis with ozonesondes and independent satellite retrievals.

The paper is structured in the following way. Section 2 describes the CAMS model and data assimilation system and gives some information about the quality of the CAMS ozone analysis fields. Section 3 looks at the Arctic stratospheric ozone field during the winter 2019/2020 and compares it with the seasons 2010/2011 and 1996/1997, and Section 4 finishes with the conclusions.

2 Data sets

2.1 The CAMS model and data assimilation system

The chemical mechanism of ECMWF's Integrated Forecast System (IFS) is a modified and extended version of the Carbon Bond 2005 chemistry scheme (CB05, Yarwood et al. 2005) chemical mechanism for the troposphere, as also implemented in the chemical transport model (CTM) TM5 (Huijnen et al., 2010). CB05 is a tropospheric chemistry scheme with 55 species and 126 reactions. Stratospheric ozone chemistry in IFS(CB05) is parameterized by a linear ozone scheme (Cariolle and Déqué, 1986; Cariolle and Teyssèdre, 2007). This combination allows a realistic representation of tropospheric and stratospheric ozone concentrations (Inness et al., 2019; Huijnen et al., 2020; Wagner et al., 2020). The chemistry module of the IFS together with its emissions are documented in more detail in Flemming et al. (2015) and Flemming et al. (2017) and the updates used in the CAMS reanalysis in Inness et al. (2019).

The IFS uses an incremental four-dimensional variational (4D-Var) data assimilation system (Courtier et al. 1994) and ozone is one of the atmospheric composition fields in the CAMS reanalysis that is included in the control vector and minimized together with the meteorological control variables. More details about the data assimilation system and background errors can be found in Inness et al. (2015) and Inness et al. (2019). Ozone retrievals from a range of satellites are assimilated in the CAMS reanalysis. These data include TCO3 retrievals from the SCanning Imaging Absorption spectroMeter for Atmospheric CHartographY (SCIAMACHY) instrument, the Ozone Monitoring Instrument (OMI) and the Global Ozone Monitoring Experiment-2 (GOME-2), ozone profile data from the Michelson Interferometer for Passive Atmospheric Sounding (MIPAS) and Microwave Limb Sounder (MLS) and partial ozone columns from Solar Backscatter ULTra-Violet (SBUV/2). More information about the assimilated ozone retrievals can be found in Inness et al. (2019). Particularly important for a realistic vertical distribution of the ozone analysis in the CAMS system is the assimilation of profile retrievals from MIPAS and MLS (Inness et al., 2013; Flemming et al., 2011; Lefever et al., 2015; Huijnen et al., 2020) that give height resolved ozone information throughout the stratosphere, including data during the polar night.

Some validation of the CAMS reanalysis is given in Inness et al. (2019). Wagner et al. (2020) present a comprehensive validation of the CAMS reanalysis against independent observations, including a detailed validation of stratospheric ozone, and Huijnen et al. (2020) provide an evaluation of tropospheric ozone for the 2003-2016 time period. There are also extensive validation reports of the CAMS reanalysis available from https://atmosphere.copernicus.eu/eqa-reports-global-services. These studies show that stratospheric ozone in the CAMS reanalysis agrees to within ±5-10 % with ozonesondes and satellite observations and does not show any discernible trends in the bias. Additional targeted

validation of the Arctic stratospheric ozone fields from the CAMS reanalysis for the period January 2003 to April 2020 is shown in the supplement and confirms that the CAMS reanalysis generally has a small negative bias (5-10%) for stratospheric ozone in the Arctic, often within the measurement uncertainties of the instruments. It gives us confidence that the CAMS reanalysis is a useful dataset to study stratospheric ozone and will allow us to describe the evolution of Arctic stratospheric ozone field during the winter and spring of 2019/2020.

2.2 ERA5 total column ozone record

The CAMS reanalysis only goes back to 2003 because most of the atmospheric composition satellite retrievals became available with the launch of the Envisat and Aura satellites in 2002 and 2004, respectively. To extend the timeseries of Arctic TCO3 back in time we use ozone columns from the ERA5 reanalysis (Hersbach et al., 2020) for the years 1979 to 2002. This reanalysis is also produced with the ECMWF IFS system and while it does not include a comprehensive tropospheric chemistry it uses the same stratospheric chemistry parameterization as the CAMS reanalysis. Therefore, stratospheric ozone or TCO3 can well be compared with the CAMS reanalysis data. In ERA5, ozone retrievals from GOME, GOME-2, MIPAS, MLS, OMI, SCIAMACHY, SBUV and the Total Ozone Mapping Spectrometer (TOMS) were assimilated as well as ozone sensitive radiances from several infrared sounders: the High-resolution Infrared Radiation Sounder (HIRS), Atmospheric Infrared Sounder (AIRS), Infrared Atmospheric Sounding Interferometer (IASI) and Cross-track Infrared Sounder (CrIS), see Hersbach et al. (2020) for more details. We restrict our use of ERA5 ozone data to TCO3 fields. These are usually well constrained by the assimilated satellite data, while vertical profiles may suffer from the lack of adequate ozone profile data during some of the years (Hersbach et al., 2020; Dragani, 2011). Hersbach et al. (2020) mention, for instance, that in the northern winter of 1996/1997, the ERA5 ozone values in the upper stratosphere at high northern latitudes are many times larger than normal, but that this problem does not significantly affect total column ozone.

Figure 1 shows the monthly mean TCO3 values for March averaged over the area north of 63ºN from the CAMS reanalysis, ERA5, the Multi Sensor Reanalysis (MSR) of total ozone (van der A, 2015) and NOAA's Merged Ozone data set (MOD; Stolarski and Frith, 2006). It shows a good agreement between ERA5, MSR and MOD data going back to 1979 with all data sets reproducing the interannual variability of TCO3 and agreeing to within 5%. ERA5 and CAMS reanalysis TCO3 values agree well for the years where the datasets overlap, but there is an increased discrepancy between ERA5 and the other datasets between 2014 and 2017. Such a positive anomaly was also noted by Hersbach et al. (2020) against a range of other reanalysis datasets and has now been traced back in part to a change from using reprocessed MLS V3 data to NRT MLS data in ERA5 at the beginning of 2015. However, we only use ERA5 data for years before 2003 and the good agreement seen between the CAMS reanalysis and ERA5 for the period 2003-2013 and between MSR, MOD and ERA5 for the earlier years gives us confidence to extend our total column dataset back in time to 1979 using ERA5 data.

Figure 1 illustrates that there is a large interannual variability in Arctic ozone in March, much of which is a result of changes in transport (both in the large scale downward transport as well as meridional mixing with midlatitudes), and a downward trend to lower ozone columns in the Arctic during the 1990s (see also WMO, 2018). The figure also shows three years with

exceptionally low Arctic ozone columns in March: 2020, 2011 and 1997. These three years will be compared in more detail in Section 3.3. Low ozone columns are generally associated with a strong polar vortex, while high values are found when the polar vortex is weak or broken up (Newman et al., 1997). The lowest values in the timeseries are found in March 2020 with average TCO3 values north of 63ºN in the CAMS reanalysis of 318 DU.

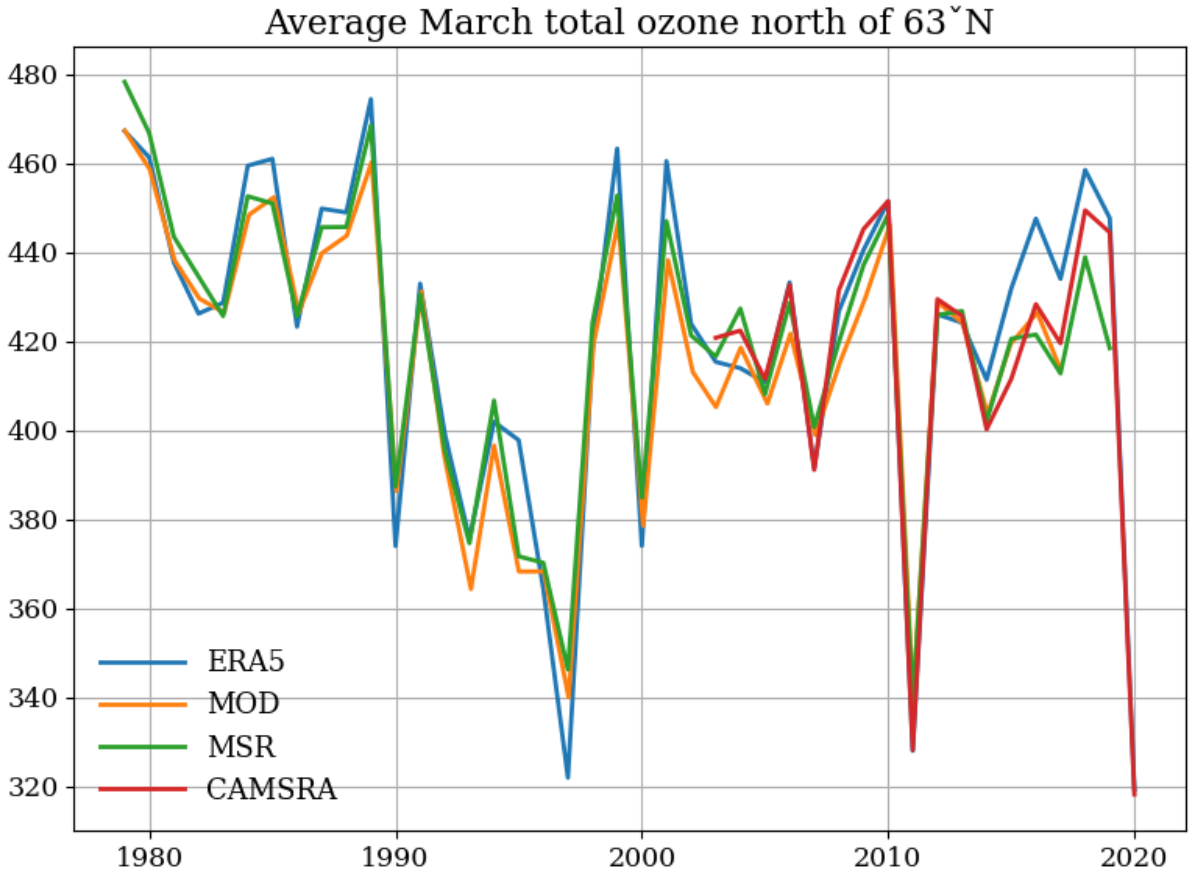

Figure 1. Timeseries of monthly mean March TCO3 in Dobson Units (DU) averaged over the area north of 63ºN from NASA's Merged Ozone data set (MOD, orange), ERA5 (blue), Multi Sensor Reanalysis (MSR, green) and CAMS reanalysis (CAMSRA, red).

3 Arctic stratospheric ozone during the winter 2019/2020

3.1 Climatological means of TCO3, temperatures and zonal winds at 50 hPa

Figure 2 shows the climatological monthly mean fields from the CAMS reanalysis (averaged over the period 2003-2019) for TCO3, temperature (T) at 50 hPa and zonal wind (U) at 50 hPa for the months December to April. The climatological TCO3 values (Figure 2a) increase from December to March with values above 450 DU in places in February and March. This spring-time maximum is the result of descent in the Arctic stratosphere during the winter

months and minimum photochemical loss during the polar night. The lowest temperatures at 50 hPa (Figure 2b) are usually found in December with values between -75ºC and -80ºC, illustrating that the climatological mean temperatures at 50 hPa in the Arctic during winter and spring are usually above the threshold for PSC formation (-78ºC). The lowest temperatures are found north of Scandinavia with values increasing from December through to April as sunlight returns to the polar regions. The low temperatures are an indication of the climatological position of the polar vortex and coincide with the lowest TCO3 values. The highest temperatures are found over Kamchatka and the Bering Sea. This coincides with the location of the highest ozone columns. During winter, the zonal winds are westerly in the stratosphere because of the large-scale meridional temperature gradient between the cold pole (no solar heating during the polar night) and the warmer mid latitudes. Figure 2c shows the belt of westerlies surrounding the North Pole that make up the polar vortex at this altitude, with the strongest zonal winds found in January and February. In an average year the polar vortex in the lower stratosphere usually forms in November, peaks in January and dissipates in early April (Coy et al., 1997). Figure 2c confirms this, showing the weakening of the zonal winds at 50 hPa from February to April, as sunlight returns to high northern latitudes and the temperature contrast between the pole and the extratropics becomes weaker. The fact that the multi-year means of TCO3, T and u are not symmetrical illustrates the impact that topography has on the circulation in the Arctic stratosphere.

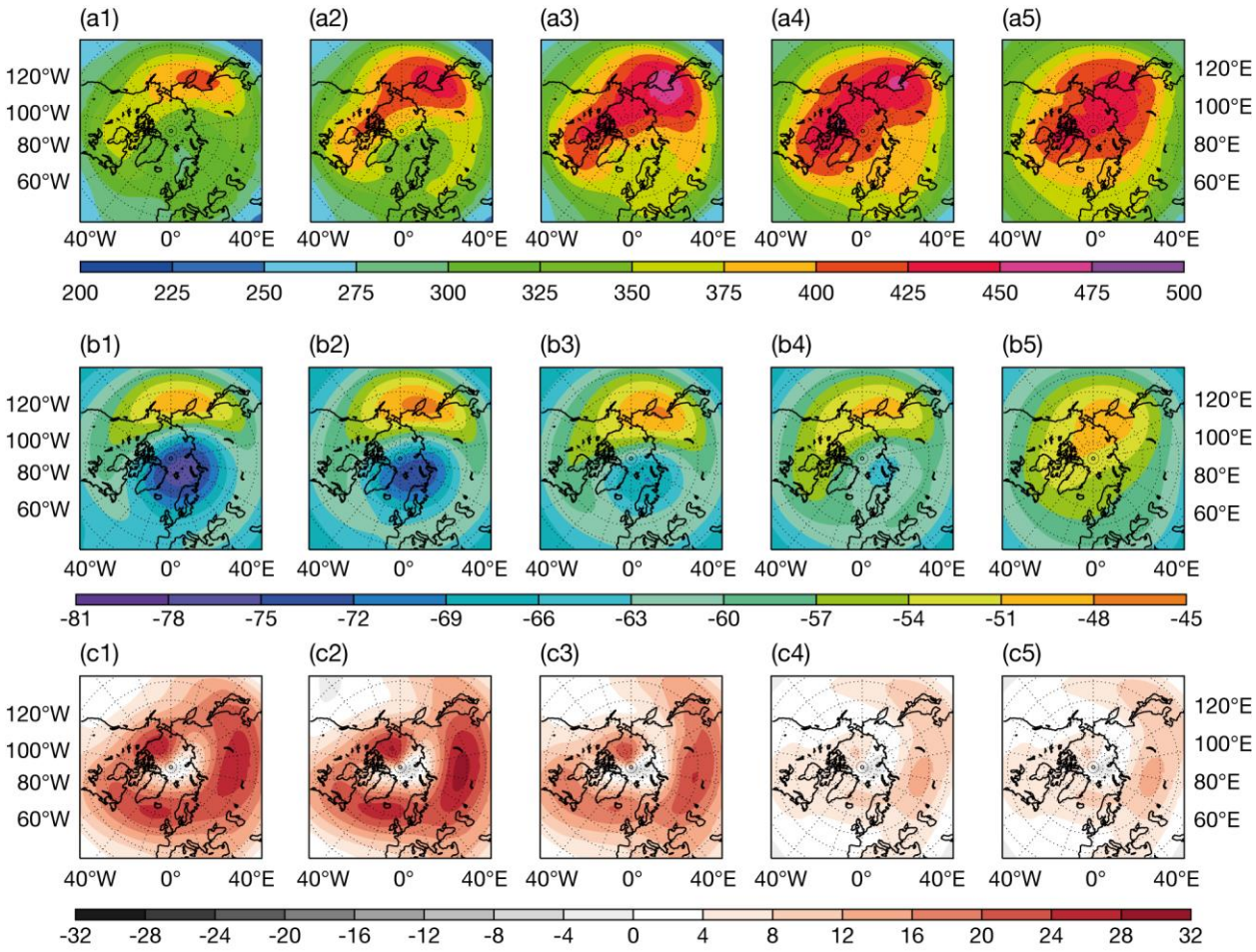

Figure 2. Climatological monthly means of (a) TCO3 (in DU), (b) temperature at 50 hPa (in ºC) and (c) zonal wind (m/s) from the CAMS reanalysis averaged over the years 2003-2019 for December (column 1), January (column 2), February (column 3), March (column 4) and April (column 5).

3.2 Anomalies of TCO3, temperatures and zonal winds at 50 hPa in 2020

Figure 3 shows timeseries of Arctic minimum TCO3 and minimum temperatures at 50 hPa (both calculated for the area north of 60ºN) from the CAMS reanalysis (2003-2020) and from ERA5 for the earlier years (1979-2002). The grey shading shows the range of the minimum values per day for the whole period 1979-2019 and the solid black line the mean values. The figure illustrates that minimum TCO3 values in the Arctic in late winter/spring show a large spread from year to year and lie between about 200 and 400 DU. Tegtmeier et al. (2008) showed that interannual variability in chemistry and the dynamical ozone supply due to transport processes (i.e. meridional mixing across vortex edge, mean transport by residual circulation and diabatic descent in polar vortex) contribute equally to the variability of Arctic wintertime TCO3. The average minimum TCO3 values increase from January to April and lie above 250 DU the whole time. In 2020 (red line in Figure 3a) the situation is completely different. While minimum

TCO3 values in January and February 2020 lie within the range of minimum values observed in other years, in March and April 2020 they are the lowest observed ozone columns in the whole record with the absolute minimum value of 211 on 18 March 2020. The previous two years with exceptionally low ozone values (2011 and 1997) are also shown in Figure 3 and will be discussed in more detail in Section 3.3 below.

The timeseries of minimum temperatures at 50 hPa (Figure 3b) shows that the lowest temperatures are found during the winter months December and January and that on average temperatures increase from January onwards as sunlight returns to the polar regions. We also see a large spread in minimum temperature values with some years having values no lower than -60ºC while others have minimum temperatures below the PSC formation threshold of -78ºC. This illustrates the large interannual variability in the Arctic stratosphere. The mean temperatures are just below the threshold for PSC formation for about two months from mid-December to early February but above it for the rest of winter and spring. Minimum temperatures in 2020 were some of the lowest in our record and below -78ºC from the beginning of January until the last week of March. This was low enough for PSCs to form and suggests that the low Arctic ozone columns seen in 2020 are at least in part the result of in-situ chemical. In particular, the low temperatures in March, when more of the vortex is illuminated by the sun, create a strong potential for catalytic ozone destruction. This will be discussed further in section 3.3. below.

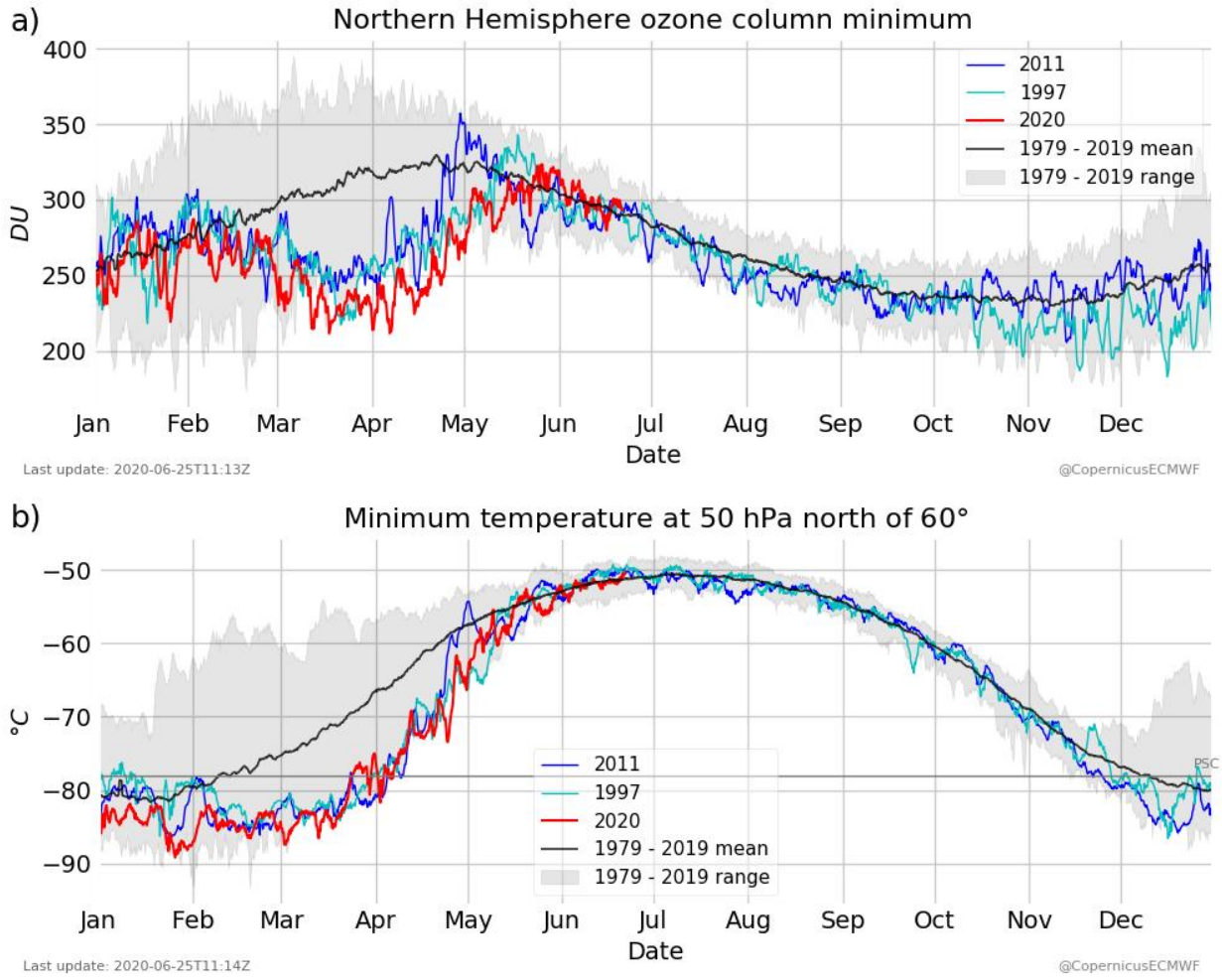

Figure 3. (a) Timeseries of minimum TCO3 (in DU) and (b) minimum temperature (in ºC) at 50 hPa north of 60ºN from CAMS reanalysis (covering the years 2003-2020) and ERA5 (1979-2002). The shaded grey area shows the range of values per day over the entire period 1979-2019, the black curve the mean values averaged over the period 1979-2019, the red curve the values for 2020, the blue curve the values for 2011 and the cyan curve the values for 1997.

Figure 4 shows the monthly mean anomalies of TCO3, T and u at 50 hPa for December 2019 to April 2020 against the climatologies from the CAMS reanalysis (Figure 2). Anomalously low TCO3 values (Figure 4a) were found over the Arctic during January to April 2020 with the largest negative anomaly of more than -180 DU seen in March 2020, about 40% below the climatological values. The negative ozone anomaly lasted well into April when TCO3 values were still more than 140 DU (or 35%) below the climatology. These ozone anomalies were associated with the anomously strong and long-lasting polar vortex illustrated by the stronger than average zonal winds at 50 hPa (Figure 4c) between January and April 2020, with the largest positive anomaly in March 2020. The polar vortex lasted well into April before it split into two around 19 April 2020. It was very stable and remained centered near the North Pole throughout, making it more akin to the polar vortex seen over Antarctic during winter/spring, and

less like the more perturbed type usually found over the Arctic. The polar vortex was considerably colder than usual throughout the winter/spring of 2020 (Figure 4b). The largest temperature anomalies at 50 hPa were found in February and March 2020, when temperatures were more than 18ºC and 21ºC, respectively, below the climatological values. The low temperatures continued into April 2020 giving the potential for catalytic ozone depletion at a time when sunlight had returned to the Arctic region.

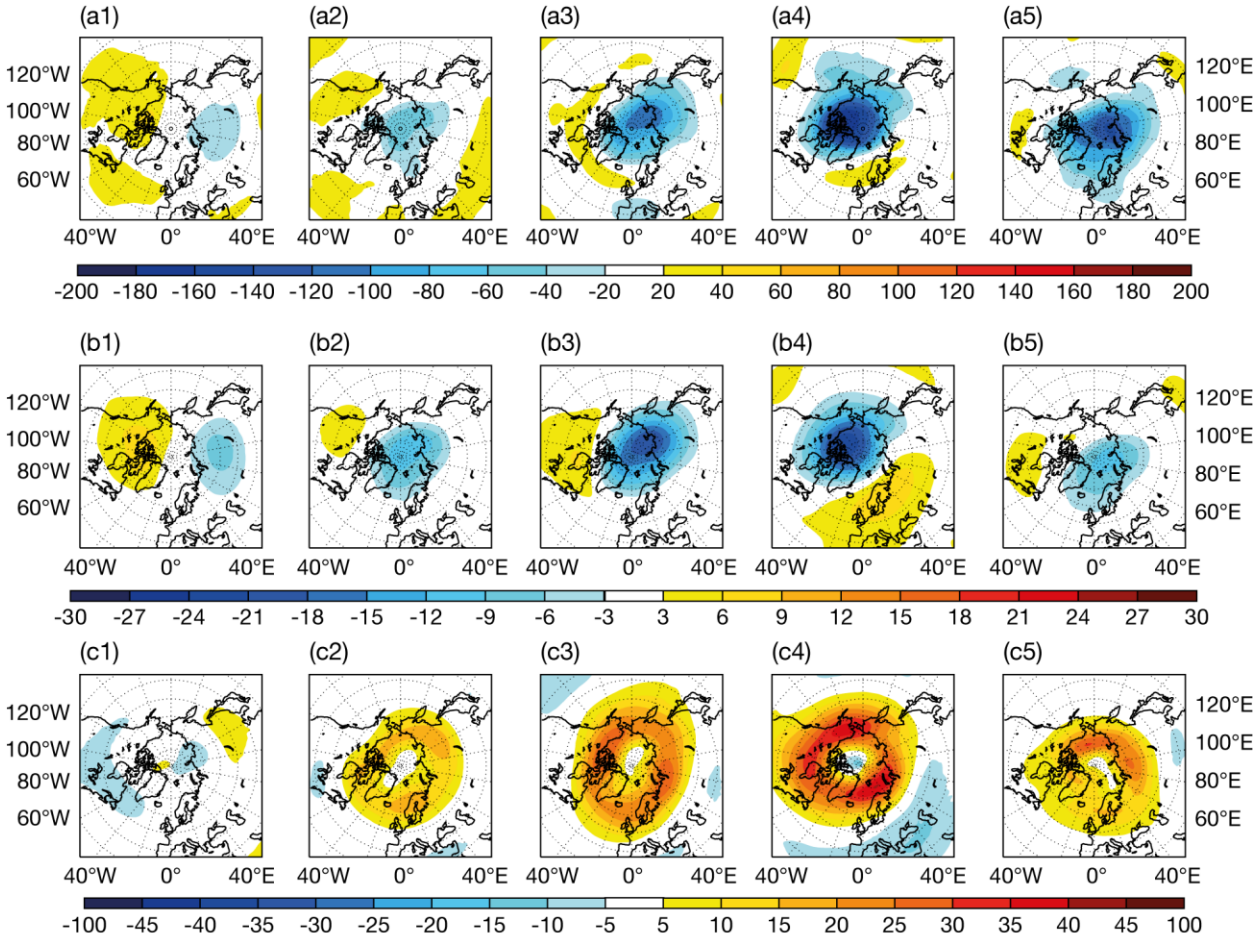

Figure 4. Monthly mean anomalies of (a) TCO3 (in DU), (b) temperature at 50 hPa (in ºC) and (c) zonal wind (m/s) from the CAMS reanalysis against the climatology calculated over the years 2003-2019 (see Figure 2) for December 2019 (column 1), January 2020 (column 2), February 2020 (column 3), March 2020 (column 4) and April 2020 (column 5).

Newman et al. (2001) showed that the temperatures of the Arctic lower stratosphere in early March are driven by the strength and duration of planetary waves propagating into the stratosphere in mid to late winter. This can be illustrated by looking at the poleward eddy heat flux in mid to late winter, a key indicator of the upward propagation of planetary waves, which is highly correlated with the mean polar stratospheric temperature during late winter. Low stratospheric temperatures are the result of weak wave forcing, and higher than average temperatures the result of strong wave forcing. Figure 5 shows the poleward 45-day running mean eddy heat flux at 50 hPa averaged between 45°N and 75°N from ERA5 for the

winter/spring 2019/2020 compared to the years from 1979 onwards. It illustrates that spring 2020 was characterized by below average planetary wave driving between January and the end of March and that values between mid-February to mid-March were below the 10th percentile of the 1979-2019 period. This low wave driving led to the large cold temperature anomalies and exceptionally strong polar vortex seen in Figure 4.

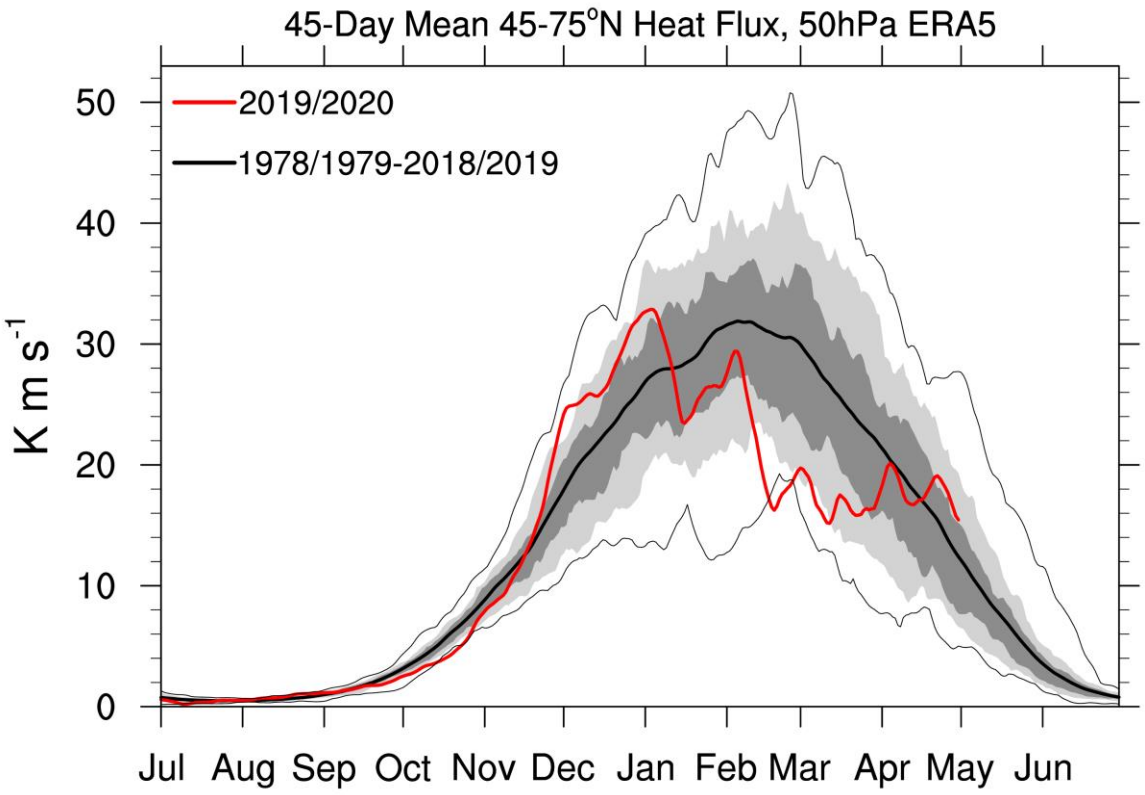

Figure 5. Eddy heat flux in Km/s at 50 hPa averaged between 45°N and 75°N for the 45-day period prior to the date indicated, calculated from ERA5 data. The light shading is the 10th to 90th percentile and the darker shading the 75-25th percentile. The thin black lines are maximum and minimum values and the red line the values for winter/spring 2019/2020.

The 3-dimensional distribution of ozone in the stratosphere as well as the corresponding vertical ozone anomalies are shown in Figure 6. Figure 6a shows cross sections of climatological monthly mean ozone partial pressure values (2003-2019) from the surface to the upper stratosphere along one meridian (0ºE/180ºE) over the North Pole. They illustrate that the ozone layer is at higher altitudes in the tropics where maximum ozone partial pressure values are found around 20 hPa and at lower altitudes over the North Pole. Figure 6a also illustrates increased ozone maximum values in the lower stratosphere in the Arctic during February and March associated with the large scale diabatic descent. The cross sections for the winter/spring months of 2020 (Figure 6b) are very different from the climatologies. In 2020, the ozone layer is considerably thinner than in the climatologies. Ozone values in the layer decrease and anomalies

against the climatology (Figure 6c) increase from January to March, and values over the North Pole remain low in April 2020.

While some of the lower ozone values were the result of reduced meridional mixing and reduce diabatic downwelling during spring 2020 as a result of reduced wave activity as seen in low eddy heat fluxes at 50 hPa (Figure 5), there is the clear signature of chemical ozone depletion (see also Figure 12 below) leading to the extremely low ozone values over the North Pole in March and April 2020. In March 2020 ozone values in the ozone layer over the North pole are reduced to around 4 mPa in the monthly mean, more than 10 mPa below the climatological values. These low values last into April 2020. The anomaly plots for 2020 (Figure 6c) illustrate the vertical extent of the ozone anomalies during spring 2020, with the largest negative anomalies found over the Arctic during March and anomalies lasting into April.

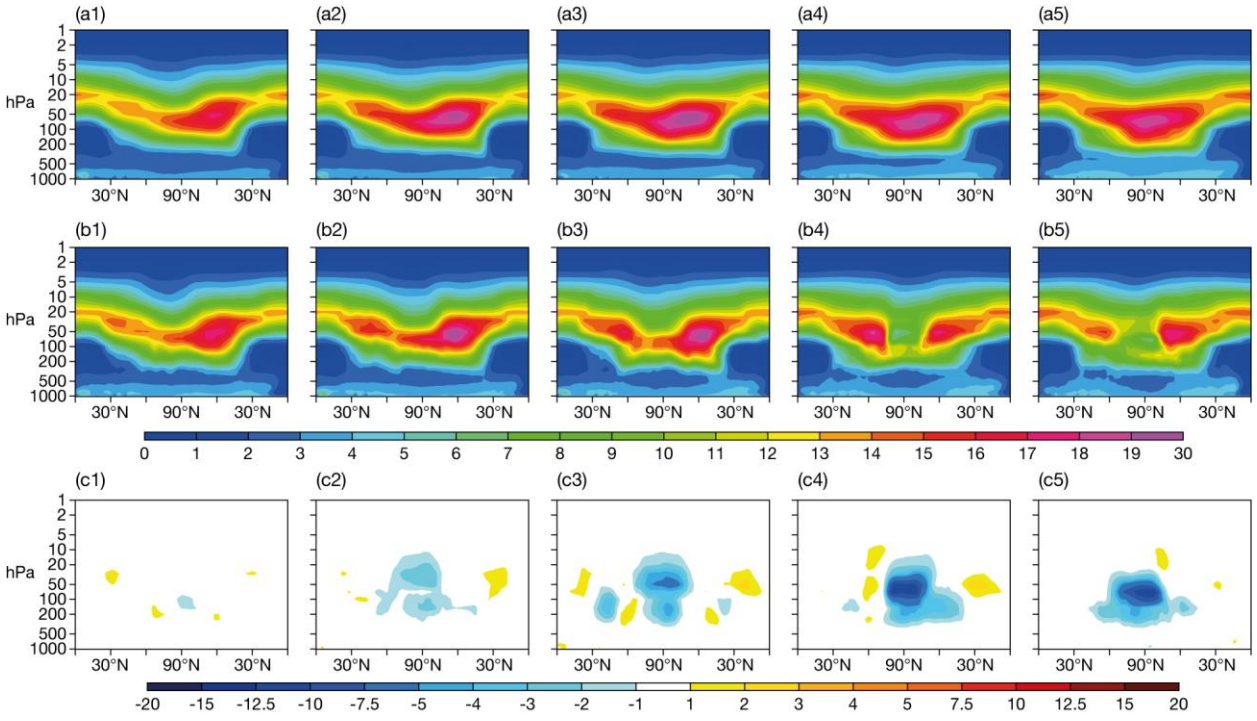

Figure 6. (a) Cross sections of monthly mean climatologically averaged ozone partial pressure (in mPa) from the CAMS reanalysis (2003-2019) along one meridian (0ºE/180ºE) from the equator north via the North Pole and back to the equator, (b) corresponding cross sections for 2019/2020 and (c) cross sections of anomalies for 2019/2020 for December (column 1), January (column 2), February (column 3), March (column 4) and April (column 5).

Figure 7 compares ozone and temperature profiles for January to April 2020 from ozone sondes at Ny-Ålesund with profiles from the CAMS reanalysis and against climatological ozone profiles. Ozone sondes are not assimilated in the CAMS reanalysis and therefore are completely independent validation data. The climatological monthly ozone profiles at Ny-Ålesund show the increase of ozone values in the lower stratosphere due to the large scale diabatic descent between January and April with a broader ozone layer and increased partial pressure values between 50 and 200 hPa. The climatological monthly means calculated from the CAMS reanalysis agree very well with sonde averages. Figure 7a shows that in 2020 the monthly mean ozone values are

lower than the climatological values in all 4 months with a narrower ozone layer in January and February 2020, which must be the result of reduced large-scale transport and associated downwelling in 2020. This is followed by a clear indication of ozone depletion in March 2020 and April 2020, when the 2020 monthly mean values are below 5 mPa between 50 and 70 hPa. Such ozone profiles are very unusual for the Arctic in boreal spring and much more akin to ozone profiles found over the Antarctic during the SH ozone hole season in October. The temperature profiles (Figure 7b) show that 2020 is considerably colder than the CAMS climatology between 30-200 hPa throughout the period, with monthly mean temperatures below -78ºC in January, February and March. Figure 8 shows four individual ozone profiles at Ny-Ålesund from the CAMS reanalysis and sondes and illustrates that in the last week of March 2020 ozone was almost completely depleted in a layer between 50 and 80 hPa, with partial pressures below 2 mPa. This layer of low ozone values remained visible in ozone sonde profiles at Ny-Ålesund until 15 April 2020 (see also Figure 11 below), while the subsequent ascent on 22 April 2020 had values between 10-18 mPa all the way between 20-200 hPa, indicating the end of the 2020 Arctic 'ozone hole' at Ny-Ålesund.

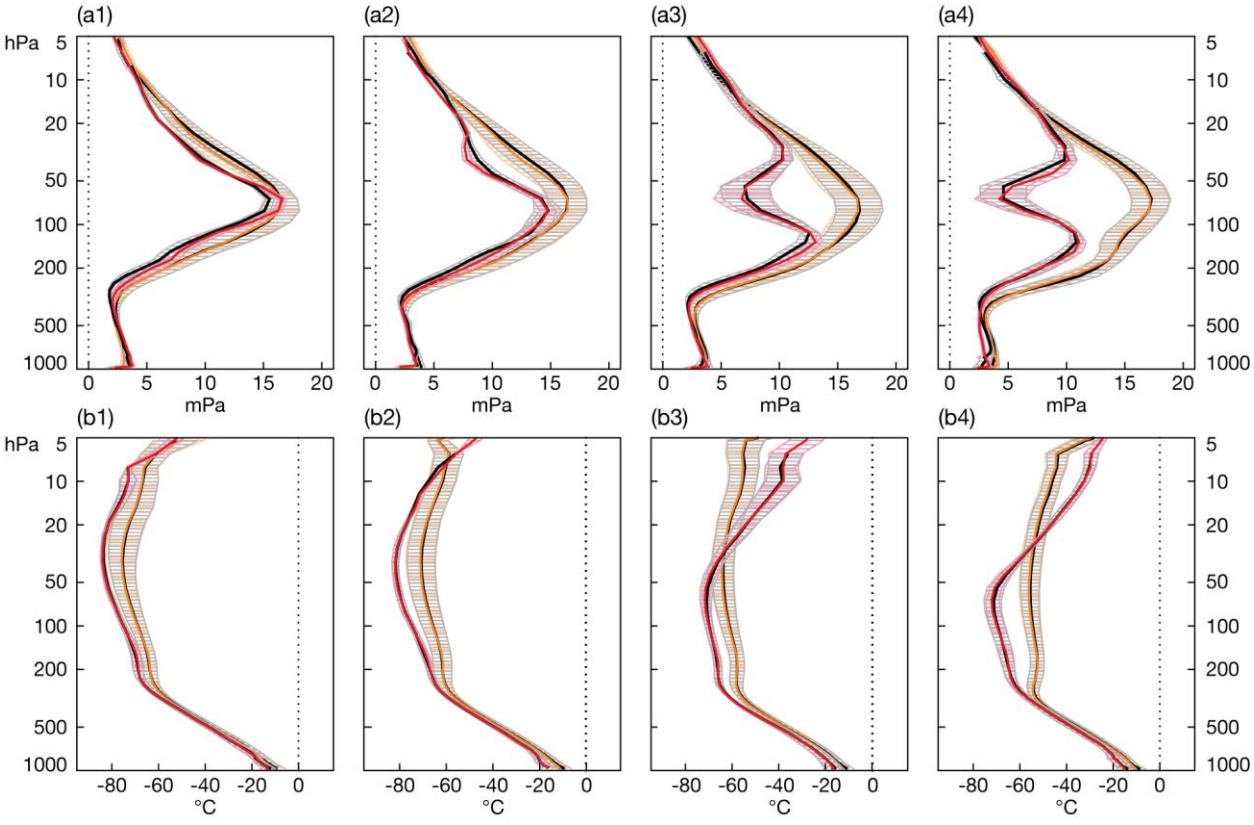

Figure 7. Comparisons of (a) ozone (in mPa) and (b) temperature (in ºC) profiles from the CAMS reanalysis and ozonesondes at Ny-Ålesund for January (column 1), February (column 2), March (column 3) and April (column 4). The red profiles show monthly mean CAMS reanalysis values for 2020, the orange profiles the climatological mean from the CAMS reanalysis (2003-2019). Black lines show the corresponding means from the ozone sondes. The hatched area depicts +/- one standard deviation. The number of ozone profiles that went into the averages

were: January 2020: 6, February 2020: 8, March 2020: 16, April 2020: 13, January climatology: 187, February climatology: 178, March climatology: 177 and April climatology: 98.

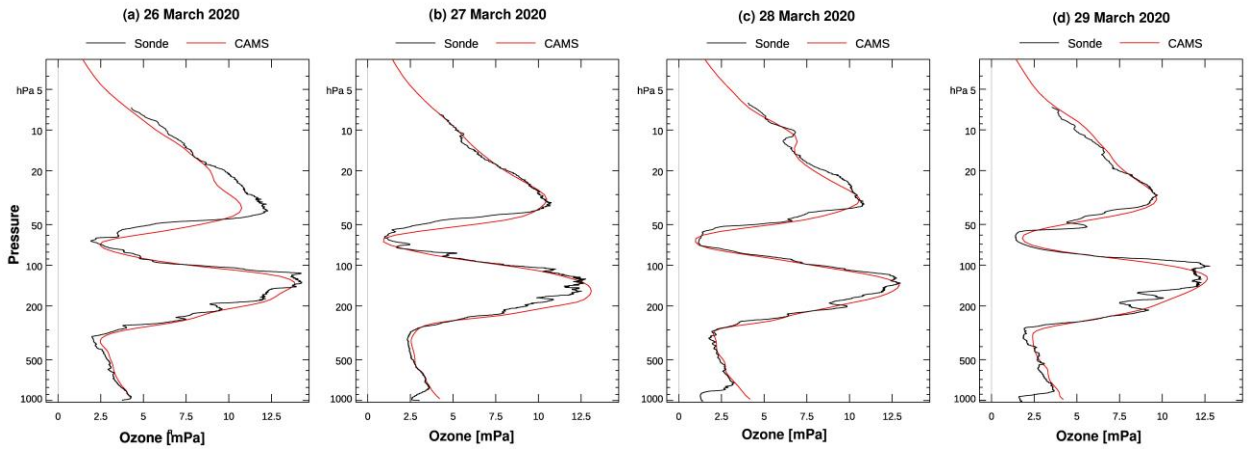

Figure 8. Ozone profiles in mPa from CAMS reanalysis (red) and ozone sondes (black) at Ny-Ålesund on (a) 26, (b) 27, (c) 28 and (d) 29 March 2020.

3.3. Comparison of Arctic ozone in spring 2020 with 2011 and 1997

The timeseries of average TCO3 north or 63ºN in Figure 1 shows how exceptionally low ozone columns over the Arctic were during March 2020 with averaged Arctic values down to 318 DU. Only two other years in the timeseries have had similarly low Arctic mean ozone values in March since 1979: 2011 with 327 DU and 1997 with 321 DU. In all three years, it was the unusual meteorological situation with a long lasting and cold polar vortex centered over the North Pole (Manney et al., 2011; Coy et al., 1997) that led to exceptional ozone losses. All three years were characterized by weak planetary wave driving from the troposphere (Newman et al., 2001; Hurwitz et al., 2011; Shaw and Perlwitz, 2014) and seen in Figure 5 for 2020. The timeseries in Figure 3a shows the daily TCO3 minimum values for 2020, 2011 and 1997 and illustrates that from late January until the end of April the minimum values in 2020 were lower than in 2011 and 1997. The lowest TCO3 minimum value in 2020 was 211 DU (on 18 March), compared to 232 DU in 2011 (on 26 February) and 217 DU in 1997 (on 21 March). The timeseries of the minimum temperatures at 50 hPa north of 60ºN (Figure 3b) shows that in 1997 temperatures were around average until early February and then fell in February. Temperatures in the first half of January 2011 were also around or above average, but in 2020 temperatures in the lower stratosphere were below average from the beginning of January and remained below the PSC formation threshold of -78ºC until the last week of March.

Figure 9 shows the monthly TCO3 anomalies for the winters 1996/97 and 2010/2011 against the CAMS climatology (using the same reference period 2003-2019). The corresponding anomalies for 2019/2020 can be found in Figure 4. All three winters had a long-lasting, cold polar vortex centered over the North Pole. However, in 1996/97 the polar vortex did not form until late December and was weaker than normal with above average temperatures until the end of January (Coy et al., 1997). The vortex was then strong and centered around the North Pole until it broke up in late April. As a result, we see positive TCO3 anomalies in December 1996 and January 1997 (Figure 9b), while in January 2020 and 2011 (Figure 9a) negative TCO3

anomalies can already be seen over the North Pole. In February, March and April large negative TCO3 anomalies are found in all three winters with the largest overall anomalies found in 2020 when values were about 27% (February), 40 % (March) and 35% (April) below the CAMS climatology. This compares with anomalies for February, March and April in 2011 of -25%, -31% and -22%, respectively, and -22%, -35% and -30% in 1997.

The situation in 2020 looks even more exceptional, especially compared to 1997, when one considers that Arctic ozone columns were at their lowest during the 1990s owing to the higher concentrations of ozone depleting substances (WMO, 2018) and have been slowly recovering (Steinbrecht et al., 2017). The lower TCO3 background values in 1997 can be seen in the negative anomalies in midlatitudes in 1996/1997 (Figure 9). Despite the lower TCO3 background values in 1997, the negative ozone anomalies against the CAMS climatology were larger in spring 2020 than 1997.

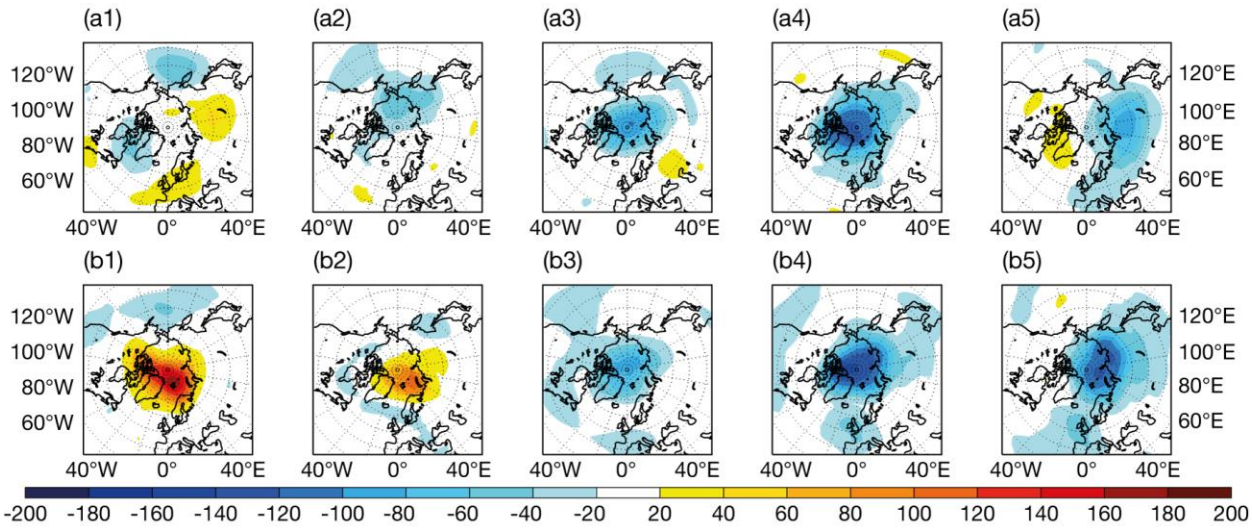

Figure 9. Monthly mean anomalies of TCO3 from (a) the CAMS reanalysis for 2010/2011 and (b) ERA 5 1996/1997 against climatologies calculated over the years 2003-2019 (see Figure 2) for December (column 1), January (column 2), February (column 3), March (column 4) and April (column 5).

In Figure 10 we compare ozone profiles at Ny-Ålesund from sondes and the CAMS reanalysis for March and April 2020 and 2011 with the CAMS climatology. The figure shows that in 2020 the exceptionally low ozone values in the lower stratosphere lasted into April, while in 2011 values had already increased again in April. Figure 11 shows timeseries of ozone profiles at Ny-Ålesund from sondes and the CAMS reanalysis for 2020 and 2011. Figure 11 shows clearly very low ozone partial pressure values in 2020 between mid-March to mid-April in the altitude range of 50-80 hPa. In 2011 low ozone partial pressure values were also seen throughout March, located at slightly higher altitude, but minimum values were not as low as in 2020. The period of very low ozone values ended at the end of March 2011 and by 4 April 2011 ozone profiles at Ny-Ålesund had values over 10 mPa everywhere between 30-200 hPa. However, this recovery did not happen until much later in 2020. An ascent at Ny-Ålesund on 15 April 2020 still showed ozone partial pressures down to 2 mPa between 60-70 hPa and only the subsequent ascent on 22 April 2020 did not show the low values any more.

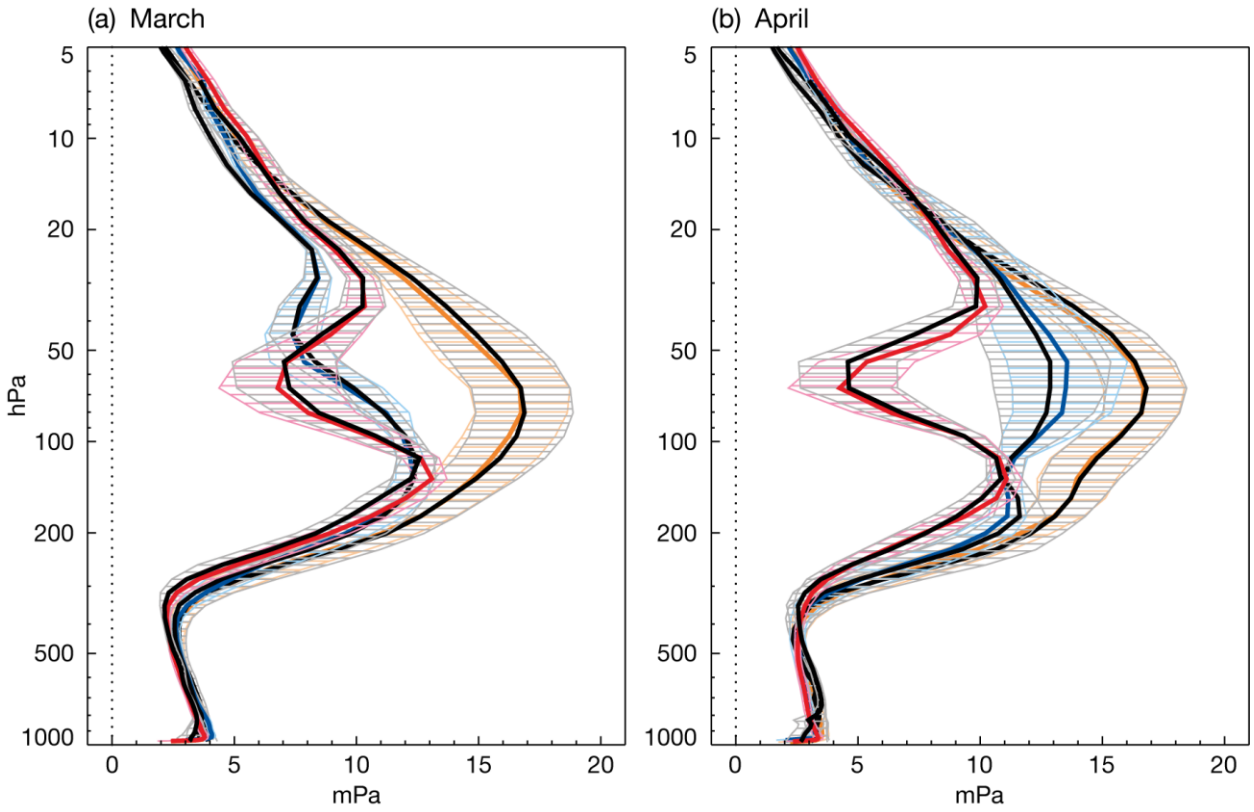

Figure 10. Monthly mean ozone profiles in mPa at Ny-Ålesund for (a) March and (b) April. The red profiles show the 2020 monthly means, the blue profiles the 2011 monthly means and the orange profiles the climatological means from the CAMS reanalysis (2003-2019). Black lines show the corresponding means from the ozone sondes. The hatched areas depict +/- one standard deviation. The number of ozone profiles that went into the averages are: March 2020: 16, March 2011: 17, March climatology: 177, April 2020: 13, April 2011: 10 and April climatology: 98.

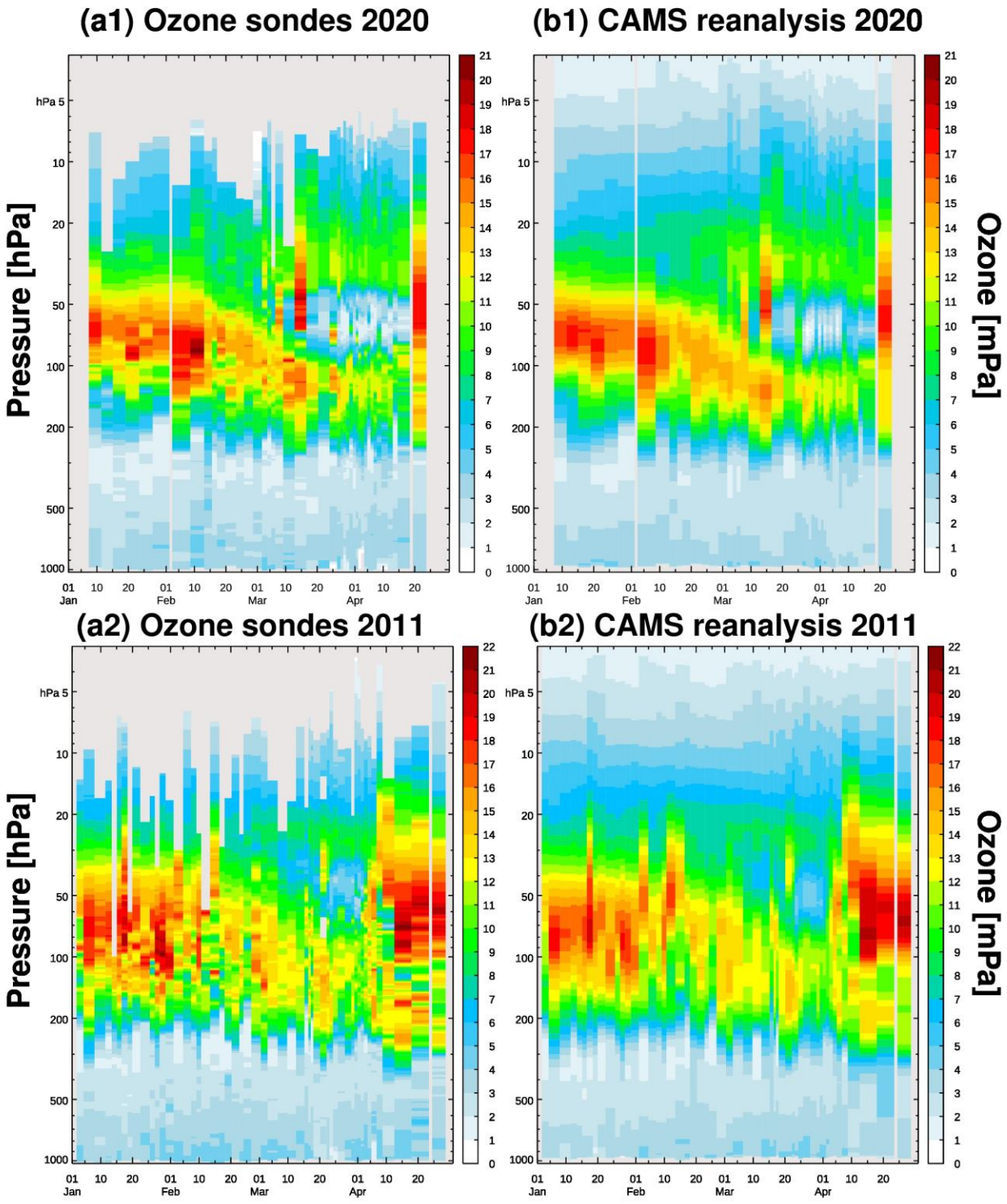

Figure 11. Timeseries from January to April of ozone profiles (in mPa) at Ny-Ålesund from ozone sondes (a) and the CAMS reanalysis (b) for 2020 (row 1) and 2011 (row 2).

Evidence that the exceptionally low ozone values seen in 2020 (and 2011) were the result of chemical ozone depletion comes from the Atmospheric Chemistry Experiment - Fourier Transform Spectrometer (ACE-FTS, Sheese et al., 2017) and MLS (Livesey et al., 2018) profiles (Figure 12). Monthly mean ASC-FTS and MLS profiles averaged over the latitude band 60-90ºN show reduced concentrations of the chlorine reservoir species hydrochloric acid (HCL) and exceptionally high abundances of chlorine monoxide (CLO) during March 2020 and 2011 relative to the ACE-FTS or MLS climatologies. There are also signs of denitrification in both years with reduced concentrations of nitric acid (HNO3). This is evidence that PSCs formed during spring 2020 (and 2011), chlorine activation happened and catalytic ozone depletion led to the very low ozone values seen during March 2020 (and 2011). Overall MLS and ACE-FTS agree very well, despite the much sparser sampling of ACE-FTS. The only exception is HNO3 where ACE-FTS indicates more HNO3 depletion in 2011 than in 2020 while MLS shows nearly the same abundances. This apparent disagreement is due to the more limited sampling in ACE-FTS, i.e. during the first half of March 2011 ACE-FTS happened to sample latitudes with very strong HNO3 depletion while MLS sampled more locations.

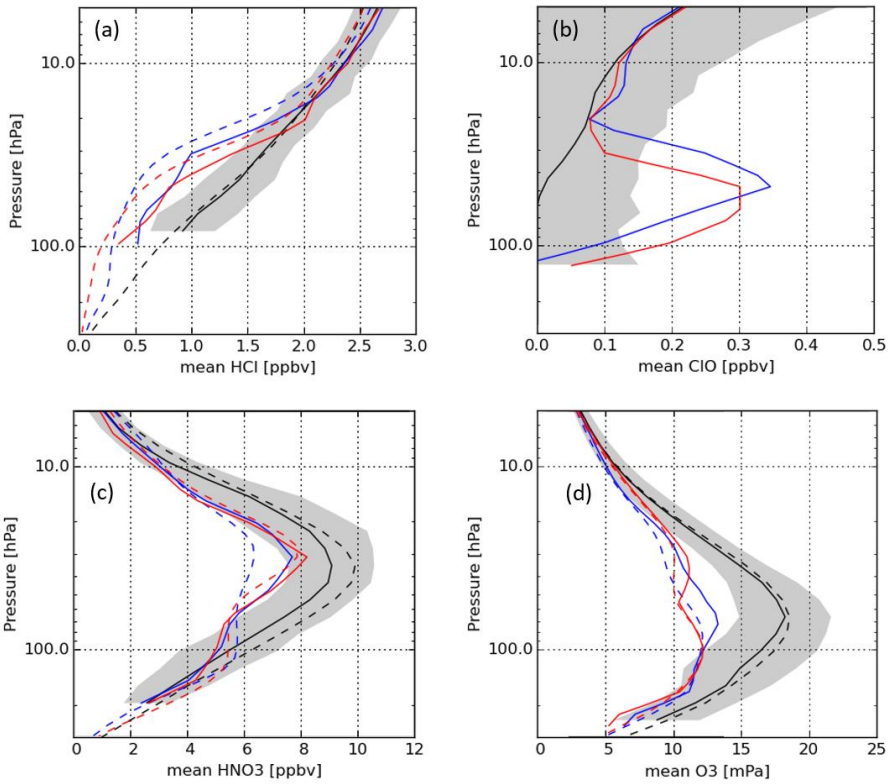

Figure 12. (a) HCL, (b) CLO, (c) HNO3, (d) ozone mean vertical profiles for March from MLS v4.2 retrievals (dashed lines) and ACE-FTS v3.6 retrievals (solid lines) and poleward of 60ºN. Shown are 2005-2019 climatologies excluding 2011 (black lines), March 2011 (blue line) and March 2020 (red lines). The grey envelopes represent two standard deviations of all profiles in each MLS climatology. All retrievals are expressed in volume mixing ratios [ppbv] except for ozone which is in partial pressure [mPa].

4 Conclusions

Data from a reanalysis of atmospheric composition produced by the Copernicus Atmosphere Monitoring Service, the so-called CAMS reanalysis, augmented by ERA5 data for years prior to 2003 were used to assess stratospheric Arctic ozone during the winter and spring of 2019/2020 and to compare it with other years since 1979. During winter and spring 2020, the Arctic polar vortex was exceptionally strong, long-lived, cold and remained centered around the North Pole until the second half of April. This was the result of weak planetary-scale wave forcing during mid to late winter. For several months, minimum temperatures in the Arctic lower stratosphere were low enough to allow the formation of PSCs, and ozone columns over large parts of the Arctic reached record low values in March and April 2020. Minimum total column ozone values were below 250 DU for most of March and the first half of April with the lowest values of 211 DU found on 18 March 2020 in the CAMS reanalysis. Such low ozone columns are extremely unusual for the NH winter/spring. They were even lower than during the previously recorded cases of large Arctic ozone depletion in 2011 and 1997 when the CAMS/ERA5 dataset had minimum values of 232 DU and 217 DU, respectively. Monthly mean Arctic TCO3 values in March 2020 were up to 180 DU or 40% lower than the CAMS climatology (calculated over the period 2003-2019) while values for 2011 and 1997 were up to 31% and 35% lower, respectively.

While some of the lower ozone values were the result of reduced diabatic downwelling and reduced meridional transport during spring 2020 because of reduced tropospheric planetary wave activity, there is evidence that chemical ozone destruction occurred and led to extremely low values in the ozone layer over the North Pole in March and April 2020. Profiles from MLS and ACE-FTS show large increases in ClO and reductions in the concentrations of HNO3 and HCl in March 2020, consistent with the presence of PSCs. Ozone profiles from sondes and the CAMS reanalysis at Ny-Ålesund show that ozone was severely depleted in a layer between 80-50 hPa where ozone partial pressure values below 2 mPa were observed at the end of March 2020. The layer of severely depleted ozone concentrations lasted until the middle of April 2020 as seen in CAMS ozone profiles and ozone sondes, longer than in 2011 when low ozone values ceased at the end of March.

The CAMS reanalysis was able to capture the exceptional Arctic ozone hole of 2020 well with good agreement between CAMS ozone profiles and independent ozone sonde data. Studies are on-going to determine why tropospheric planetary wave forcing was so weak in winter/spring 2020 and if there was any feedback from the Arctic ozone depletion onto the dynamics that helped to prolong the strong vortex. An interesting question would also be to investigate whether and to what extent ash and SO_2 that were injected into the Arctic stratosphere after the Raikoke eruption in June 2019 helped to enhance PSC formation and the subsequent ozone depletion in the Arctic during spring 2020. It remains to be seen if this kind of Arctic ozone hole will continue to be an exceptional event or occur more often in a changing climate.

Acknowledgments, Samples, and Data

The Copernicus Atmosphere Monitoring Service is operated by the European Centre for Medium-Range Weather Forecasts on behalf of the European Commission as part of the Copernicus programme (http://copernicus.eu). CAMS reanalysis data are freely available from the CAMS Atmosphere Data Store (ADS, https://ads.atmosphere.copernicus.eu/cdsapp#!/home) and ERA5 data are available from the Climate Data Store (CDS,

https://cds.climate.copernicus.eu/#!/home). Thanks to Luke Jones for providing the tools for the validation against ozone sondes and to Anabel Bowen for improving some of the figures.

Thanks to the data providers of the data assimilated in the CAMS reanalysis and the data used for the validation studies in this paper. The FTIR data used in this publication were obtained as part of the Network for the Detection of Atmospheric Composition Change (NDACC) and are publicly available (see http://www.ndacc.org). The MSR data was downloaded from the Temis website (http://www.temis.nl). ACE-FTS is an instrument of the Canadian-led Atmospheric Chemistry Experiment (also known as SCISAT) that is mainly supported by the CSA and NSERC. We acknowledge the MLS mission scientists and associated NASA personnel for the production of the data used in this study. The ozone sondes at Ny-Ålesund were launched by the Alfred-Wegener-Institut Helmholtz-Zentrum für Polar- und Meeresforschung (AWI).

References

Brewer, A. W. (1949), Evidence for a world circulation provided by measurements of helium and water vapour distribution in the stratosphere, *Q. J. R. Meteorol. Soc.*, 75, 351, doi:10.1002/qj.49707532603

Cariolle, D. and Déqué, M. (1986), Southern hemisphere medium-scale waves and total ozone disturbances in a spectral general circulation model, *J. Geophys. Res., 91,* 10825–10846

Cariolle, D. and Teyssèdre, H. (2007), A revised linear ozone photochemistry parameterization for use in transport and general circulation models: multi-annual simulations, *Atmos. Chem. Phys.*, 7, 2183–2196, https://doi.org/10.5194/acp-7-2183-2007

Courtier, P., Thépaut, J.-N., and Hollingsworth, A. (1994), A strategy for operational implementation of 4D-Var, using an incremental approach, *Q. J. Roy. Meteor. Soc.*, 120, 1367–1388

Coy L., P. A. Newman, and E. R. Nash (1997), Meteorology of the polar vortex: March 1997, *Geophys. Res. Lett.*, Vol. 24, No. 22, 2693-2696.

Dee, D. P. and Uppala, S. (2009): Variational bias correction of satellite radiance data in the ERA-Interim reanalysis, *Q. J. Roy. Meteor. Soc.*, 135, 1830–1841

Dobson, G. M. G. (1956), Origin and distribution of polyatomic molecules in the atmosphere, *Proc. R. Soc. Lond. A.*, 236, 187–193

Dragani, R. (2011): On the quality of the ERA-Interim ozone reanalyses:comparisons with satellite data, *Q. J. Roy. Meteor. Soc.*, 137,1312–1326, oi:http://dx.doi.org/10.1002/qj.82110.1002/qj.821,

Flemming, J., Inness, A., Jones, L., Eskes, H. J., Huijnen, V., Schultz, M. G., Stein, O., Cariolle, D., Kinnison, D., and Brasseur, G. (2011): Forecasts and assimilation experiments of the Antarctic ozone hole 2008, *Atmos. Chem. Phys.*, 11, 1961–1977, https://doi.org/10.5194/acp-11-1961-2011

Flemming, J., Huijnen, V., Arteta, J., Bechtold, P., Beljaars, A., Blechschmidt, A.-M., Diamantakis, M., Engelen, R. J., Gaudel, A., Inness, A., Jones, L., Josse, B., Katragkou, E., Marecal, V., Peuch, V.-H., Richter, A., Schultz, M. G., Stein, O., and Tsikerdekis, A.

(2015), Tropospheric chemistry in the Integrated Forecasting System of ECMWF, *Geosci. Model Dev.*, 8, 975–1003, https://doi.org/10.5194/gmd-8-975-2015

Flemming, J., Benedetti, A., Inness, A., Engelen, R. J., Jones, L., Huijnen, V., Remy, S., Parrington, M., Suttie, M., Bozzo, A., Peuch, V.-H., Akritidis, D., and Katragkou, E. (2017): The CAMS interim Reanalysis of Carbon Monoxide, Ozone and Aerosol for 2003–2015, *Atmos. Chem. Phys.*, 17, 1945–1983, https://doi.org/10.5194/acp-17-1945-2017

Garcia, R. R., and Boville, B. A. (1994): "Downward Control" of the Mean Meridional Circulation and Temperature Distribution of the Polar Winter Stratosphere, J. Atmos. Sci., 51, 2238–2245, https://doi.org/10.1175/1520-0469(1994)051<2238:COTMMC>2.0.CO;2

Hersbach, H., Bell, B., Berrisford, P., Hirahara, S., Horanyi, A., Munoz-Sabater, J., Nicolas, J., Peubey, C., Radu, R., Schepers, D., Simmons, A., Soci, C., Abdallaa, S., Abellan, X., Balsamo, G., Bechtold, P., Biavati, G., Bidlot, J., Bonavita, M., De Chiara, G., Dahlgren, P., Dee, D., Diamantakis, M., Dragani, R., Flemming, J., Forbes, R., Fuentes, M., Geer, A., Haimberger, L., Healy, S., Hogan, R.J., Holm, E., Janiskova, M., Keeley, S., Laloyaux, P., Lopez, P., Radnoti, G., de Rosnay, P., Rozum, I., Vamborg, F., Villaume, S., Thepaut, J.N. (2020), The ERA5 Global Reanalysis, *Quarterly Journal of the Royal Meteorological Society*, https://rmets.onlinelibrary.wiley.com/doi/abs/10.1002/qj.3803

Hubert, D., Lambert, J.-C., Verhoelst, T., Granville, J., Keppens, A., Baray, J.-L., Bourassa, A. E., Cortesi, U., Degenstein, D. A., Froidevaux, L., Godin-Beekmann, S., Hoppel, K. W., Johnson, B. J., Kyrölä, E., Leblanc, T., Lichtenberg, G., Marchand, M., McElroy, C. T., Murtagh, D., Nakane, H., Portafaix, T., Querel, R., Russell III, J. M., Salvador, J., Smit, H. G. J., Stebel, K., Steinbrecht, W., Strawbridge, K. B., Stübi, R., Swart, D. P. J., Taha, G., Tarasick, D. W., Thompson, A. M., Urban, J., van Gijsel, J. A. E., Van Malderen, R., von der Gathen, P., Walker, K. A., Wolfram, E., and Zawodny, J. M. (2016), Ground-based assessment of the bias and long-term stability of 14 limb and occultation ozone profile data records, *Atmos. Meas. Tech.*, 9, 2497–2534, https://doi.org/10.5194/amt-9-2497-2016

Huijnen, V., Williams, J., van Weele, M., van Noije, T., Krol, M., Dentener, F., Segers, A., Houweling, S., Peters, W., de Laat, J., Boersma, F., Bergamaschi, P., van Velthoven, P., Le Sager, P., Eskes, H., Alkemade, F., Scheele, R., Nédélec, P., and Pätz, H.-W. (2010), The global chemistry transport model TM5: description and evaluation of the tropospheric chemistry version 3.0, *Geosci. Model Dev.*, 3, 445–473, https://doi.org/10.5194/gmd-3-445-2010

Huijnen, V., Miyazaki, K., Flemming, J., Inness, A., Sekiya, T., and Schultz, M. G.: An intercomparison of tropospheric ozone reanalysis products from CAMS, CAMS interim, TCR-1, and TCR-2, *Geosci. Model Dev.*, 13, 1513–1544, https://doi.org/10.5194/gmd-13-1513-2020, 2020.

Hurwitz, M. M., P. A. Newman, and C. I. Garfinkel (2011): The Arctic vortex in March 2011: Adynamical perspective. *Atmos.Chem. Phys.*, 11, 11 447–11 453.

Inness, A., Baier, F., Benedetti, A., Bouarar, I., Chabrillat, S., Clark, H., Clerbaux, C., Coheur, P., Engelen, R. J., Errera, Q., Flemming, J., George, M., Granier, C., Hadji-Lazaro, J.,

Huijnen, V., Hurtmans, D., Jones, L., Kaiser, J. W., Kapsomenakis, J., Lefever, K., Leitão, J., Razinger, M., Richter, A., Schultz, M. G., Simmons, A. J., Suttie, M., Stein, O., Thépaut, J.-N., Thouret, V., Vrekoussis, M., Zerefos, C., and the MACC team (2013): The MACC reanalysis: an 8 yr data set of atmospheric composition, *Atmos. Chem. Phys.*, 13, 4073–4109, https://doi.org/10.5194/acp-13-4073-2013

Inness, A., Blechschmidt, A.-M., Bouarar, I., Chabrillat, S., Crepulja, M., Engelen, R. J., Eskes, H., Flemming, J., Gaudel, A., Hendrick, F., Huijnen, V., Jones, L., Kapsomenakis, J., Katragkou, E., Keppens, A., Langerock, B., de Mazière, M., Melas, D., Parrington, M., Peuch, V. H., Razinger, M., Richter, A., Schultz, M. G., Suttie, M., Thouret, V., Vrekoussis, M., Wagner, A., and Zerefos, C. (2015): Data assimilation of satellite-retrieved ozone, carbon monoxide and nitrogen dioxide with ECMWF's Composition-IFS, *Atmos. Chem. Phys.*, 15, 5275–5303, https://doi.org/10.5194/acp-15-5275-2015

Inness, A., Ades, M., Agustí-Panareda, A., Barré, J., Benedictow, A., Blechschmidt, A.-M., Dominguez, J. J., Engelen, R., Eskes, H., Flemming, J., Huijnen, V., Jones, L., Kipling, Z., Massart, S., Parrington, M., Peuch, V.-H., Razinger, M., Remy, S., Schulz, M., and Suttie, M. (2019), The CAMS reanalysis of atmospheric composition, *Atmos. Chem. Phys.*, 19, 3515–3556, https://doi.org/10.5194/acp-19-3515-2019

Komhyr, W. D., Barnes, R. A., Borthers, G. B., Lathrop, J. A., Kerr, J. B., and Opperman, D. P. (1995): Electrochemical concentration cell ozonesonde performance evaluation during STOIC 1989, *J. Geophys. Res.*, 100, 9231–9244

Laeng,A., von Clarmann, T., Stiller, G., Grabowski, U., Kiefer, M., Hubert, D., Verhoelst, T., Keppens, A., Lambert, J. C., Dinelli, B. M., Dudhia, A., Raspollini, P., Sofieva, V., Froidevaux, L., Walker, K. A., Zehner, C. (2018), The ozone climate change initiative: Comparison of four Level-2 processors for the Michelson Interferometer for Passive Atmospheric Sounding (MIPAS), Remote Sensing of Environment, ISSN: 0034-4257, Vol: 162, Page: 316-343, https://doi.org/10.1016/j.rse.2014.12.013

Langerock, B., De Mazière, M., Hendrick, F., Vigouroux, C., Desmet, F., Dils, B., and Niemeijer, S. (2015), Description of algorithms for co-locating and comparing gridded model data with remote-sensing observations, *Geosci. Model Dev.*, 8, 911–921, https://doi.org/10.5194/gmd-8-911-2015, 2015.

Lawrence, A. D., Perlwitz, J., Butler, A. H., Manney, G. L., Newman, P. A., Lee, S. H. and Nash, E. R. (2020), The Remarkably Strong Arctic Stratospheric Polar Vortex of Wnter 2020: Links to Record-Breaking Arctic Oscillation and Ozone Loss, Submitted to *J. Geophys. Res.*, https://doi.org/10.1002/essoar.10503356.1

Lefever, K., van der A, R., Baier, F., Christophe, Y., Errera, Q., Eskes, H., Flemming, J., Inness, A., Jones, L., Lambert, J.-C., Langerock, B., Schultz, M. G., Stein, O., Wagner, A., and Chabrillat, S. (2015), Copernicus stratospheric ozone service, 2009–2012: validation, system intercomparison and roles of input data sets, *Atmos. Chem. Phys.*, 15, 2269–2293, https://doi.org/10.5194/acp-15-2269-2015

Livesey, N J., Read, William G., Wagner, P. A., Froidevaux, L., Lambert, A., Manney, G. L., Millán, L. F., Valle, H. C. Pumphrey, M. L., Santee, M. J., Schwartz, S. W., Fuller, R. A., Jarnot, R. F., Knosp, B. W., Martinez, E., Lay, R. R. (2018): Version 4.2x Level 2 data

quality and description document, Tech. rep. , Jet Propulsion Laboratory, available from http://mls.jpl.nasa.gov/.

Manney, G., Zurek, R. W., O'Neill, A. and Swinbank, R. (1994): On the Motion of Air through the Stratospheric Polar Vortex, J. Atmos. Sci., 51, 2973–2994, https://doi.org/10.1175/1520-0469(1994)051<2973:OTMOAT>2.0.CO;2.

Manney, G., Santee, M., Rex, M. et al. (2011), Unprecedented Arctic ozone loss in 2011. *Nature*, 478, 469–475. https://doi.org/10.1038/nature10556

McPeters, R. D., Bhartia, P. K., Haffner, D., Labow, G. J., and Flynn, L. (2013): The version 8.6 SBUV ozone data record: An overview, *J. Geophys. Res.-Atmos.*, 118, 8032–8039, https://doi.org/10.1002/jgrd.50597

Newman, P. A., E. R. Nash, and J. E. Rosenfield (2001), What controls the temperature in the Arctic stratosphere in the spring? *J. Geophys. Res*., 106 (D17), 19 999–20 010.

Newman, P. A., J. F. Gleason, and R. S. Stolarski (1997), Anomalously low ozone over the Arctic, *Geophys. Res. Lett.*, Vol. 24, No. 22, 2689-2692.

Sheese, P. E., Walker, K. A., Boone, C. D., Bernath, P. F., Froidevaux, L., Funke, B., Raspollini, P., von Clarmann, T. (2015), ACE-FTS ozone, water vapour, nitrous oxide, nitric acid, and carbon monoxide profile comparisons with MIPAS and MLS, Journal of Quantitative Spectroscopy and Radiative Transfer, Volume 186, January 2017, Pages 63-80, https://doi.org/10.1016/j.jqsrt.2016.06.026

Shepherd, T. G. (2008), Dynamics, stratospheric ozone, and climate change, *Atmosphere-Ocean*, 46:1, 117-138, DOI: 10.3137/ao.460106

Stauffer, R. M., Thompson, A. M., Kollonige, D. E., Witte, J. C., Tarasick, D. W., Davies, J., et al. (2020). A post-2013 dropoff in total ozone at a third of global ozonesonde stations: Electrochemical concentration cell instrument artifacts? *Geophysical Research Letters*, 47, https://doi.org/10.1029/2019GL086791

Steinbrecht, W., Froidevaux, L., Fuller, R., Wang, R., Anderson, J., Roth, C., Bourassa, A., Degenstein, D., Damadeo, R., Zawodny, J., Frith, S., McPeters, R., Bhartia, P., Wild, J., Long, C., Davis, S., Rosenlof, K., Sofieva, V., Walker, K., Rahpoe, N., Rozanov, A., Weber, M., Laeng, A., von Clarmann, T., Stiller, G., Kramarova, N., Godin-Beekmann, S., Leblanc, T., Querel, R., Swart, D., Boyd, I., Hocke, K., Kämpfer, N., Maillard Barras, E., Moreira, L., Nedoluha, G., Vigouroux, C., Blumenstock, T., Schneider, M., García, O., Jones, N., Mahieu, E., Smale, D., Kotkamp, M., Robinson, J., Petropavlovskikh, I., Harris, N., Hassler, B., Hubert, D., and Tummon, F. (2017), An update on ozone profile trends for the period 2000 to 2016, *Atmos. Chem. Phys.*, 17, 10675–10690, https://doi.org/10.5194/acp-17-10675-2017

Steinbrecht, W., Shwartz, R., and Claude, H. (1998), New pump correction for the Brewer-Mast ozonesonde: Determination from experiment and instrument intercomparisons, *J. Atmos. Ocean. Tech.*, 15, 144–156

Stolarski, R. S. and Frith, S. M. (2006), Search for evidence of trend slow-down in the long-term TOMS/SBUV total ozone data record: the importance of instrument drift uncertainty, Atmos. Chem. Phys., 6, 4057–4065, https://doi.org/10.5194/acp-6-4057-2006.

Tegtmeier, S., Rex, M., Wohltmann, I. & Krüger, K. (2008), Relative importance of dynamical and chemical contributions to Arctic wintertime ozone. *Geophys. Res. Lett.,* Vol. 35, L17801 http://dx.doi.org/10.1029/2008GL034250

van der A, R. J., Allaart, M. A. F., and Eskes, H. J.: Extended and refined multi sensor reanalysis of total ozone for the period 1970–2012 (2015), *Atmos. Meas. Tech.*, 8, 3021–3035, https://doi.org/10.5194/amt-8-3021-2015.

Wagner et al. (2020): Comprehensive Evaluation of the Copernicus Atmosphere Monitoring Service (CAMS) reanalysis against independent observations. Submitted to Elementa: Science of the Anthropocene, www.elementascience.org

Waugh, D.W, A Sobel, L.M. Polvani (2017), What is the Polar Vortex and how does it influence weather? *Bulletin of the American Meteorological Society*, 98, 37-44. doi.org/10.1175/BAMS-D-15-00212.1

WMO (World Meteorological Organization), Scientific Assessment of Ozone Depletion: 2018, Global Ozone Research and Monitoring Project – Report No. 58, 588 pp., Geneva, Switzerland, 2018.

Yarwood, G., Rao, S., Yocke, M., and Whitten, G. (2005), Updates to the carbon bond chemical mechanism: CB05, Final report to the US EPA, *EPA Report Number*: RT-0400675, available at: http://www.camx.com